Running title: *Brain rhythms and human vision*
Revised manuscript to: *International Journal of Psychophysiology*
Date: 8th December 2010

Manuscript # CCD766

The role of oscillatory brain activity in object processing and figure-ground segmentation in human vision

K. Kinsey[ab†], S.J. Anderson[a], A. Hadjipapas[a] and I.E. Holliday[a]

[a]School of Life and Health Sciences, Aston University,
The Wellcome Trust Laboratory for MEG Studies, Birmingham, B4 7ET, UK
[b]School of Life and Health Sciences, Dept. of Psychology, University of the West of England, Bristol, BS16, 1QY, UK

Correspondence: Dr K. Kinsey *(kris.kinsey@uwe.ac.uk)*
[†]Current address: Department of Psychology, School of Life and Health Sciences, University of the West of England, Frenchay Campus, Bristol, BS16 1QY, UK.

Figures: 6
Word count: 6347 (excluding references and figure captions)
Keywords: MEG, SAM, vision, object-recognition, gamma, figure-ground, binding

Abstract

The perception of an object as a single entity within a visual scene requires that its features are bound together and segregated from the background and/or other objects. Here, we used magnetoencephalography (MEG) to assess the hypothesis that coherent percepts may arise from synchronized high frequency (gamma) activity between neurons that code features of the same object. We also assessed the role of low frequency (alpha, beta) activity in object processing. The target stimulus (i.e. object) was a small patch of a concentric grating of 3 c/deg, viewed eccentrically. The background stimulus was either a blank field or a concentric grating of 3 c/deg periodicity, viewed centrally. With patterned backgrounds, the target stimulus emerged – through rotation about its own centre – as a circular subsection of the background. Data were acquired using a 275-channel whole-head MEG system and analyzed using Synthetic Aperture Magnetometry (SAM), which allows one to generate images of task-related cortical oscillatory power changes within specific frequency bands. Significant oscillatory activity across a broad range of frequencies was evident at the V1/V2 border, and subsequent analyses were based on a virtual electrode at this location. When the target was presented in isolation, we observed: (i) contralateral stimulation yielded a sustained power increase in gamma activity; (ii) both contra- and ipsilateral stimulation yielded near identical transient power changes in alpha (and beta) activity. When the target was presented against a patterned background, we observed: (i) contralateral stimulation yielded an increase in high-gamma (> 55 Hz) power together with a decrease in low-gamma (40-55 Hz) power; (ii) both contra- and ipsilateral stimulation yielded a transient decrease in alpha (and beta) activity, though the reduction tended to be greatest for contralateral stimulation. The opposing power changes across different regions of the gamma spectrum with ‘figure/ground’ stimulation suggest a possible dual role for gamma rhythms in visual object coding, and provide general support of the binding-by-synchronization hypothesis. As the power changes in alpha and beta activity were largely independent of the spatial location of the target, however, we conclude that their role in object processing may relate principally to changes in visual attention.

1. **Introduction**

Although the primate brain contains over 30 distinct visual areas (Van Essen, 2004), we experience a unified perceptual view of the world in the blink of an eye. How the brain executes this feat of combining information across spatially separate areas with millisecond precision, rendering our visual world stable and whole, remains an open question. A solution to 'the binding problem', as it has come to be known, is keenly sought not only because it may lead to a significant increase in our understanding of visual processing but also because it may provide some insight into consciousness itself (Crick, 1994). Assuming that activity in disparate cortical areas must be grouped at some stage of processing – for it is difficult to imagine how a coherent percept could be achieved otherwise – the choice of binding solutions appears limited to one based on hierarchical processing and/or co-ordinated activity among distributed cortical areas. It is clear that hierarchical processing must play some role in the formation of coherent percepts, for it is known from the pioneering work of Hubel and Wiesel (1962, 1968) and others that large sections of the visual system are organised in just such a manner. However, a binding solution based entirely on hierarchical (feedforward) processing is not feasible as the number of neurons required to process each unique view of every object would be unacceptably large. Moreover, such a theory disregards the multitude of feedback projections within the visual system that may be vital for the generation of global percepts (Bullier, 2001; Halgren, Mendola, Chong, & Dale, 2003; Thielscher, Kolle, Neumann, Spitzer, & Gron, 2008)

More recently, it has been hypothesized that coherent percepts may arise from synchronized spike activity between neurons that code features of the same object. The binding-by-synchronization model, which attributes roles to both feedforward and feedback processes, has been advanced largely on the basis of animal studies (Eckhorn, et al., 1988; Gray & Singer, 1989; Kreiter & Singer, 1996; W Singer, 2007). Our goal in this paper was to make use of the spatio-temporal resolution offered by the neuroimaging technique of magnetoencephalography (MEG) to assess the synchronization model of object processing in human vision. What follows is a brief overview of cortical oscillatory activity and its possible role in neural binding, and a rationale for the protocols used in our study.

1.1 Cortical oscillations and visual binding

The cortical process whereby several object features are represented as a whole, removed from bound features of other objects, is critical for the emergence of a unified

perceptual view of the world. Phenomenologically, this grouping and segregation is described within a Gestalt framework as 'figure-ground' perception. The binding-by-synchronization hypothesis holds that grouping and segmenting information operates through a neural mechanism whereby visual features coded across distributed neuronal assemblies are represented as components of a common object through synchronous oscillatory firing patterns (Eckhorn, et al., 2004; Gail, Brinksmeyer, & Eckhorn, 2000; W. Singer, 1999). For example, neurons in the visual cortex show synchronous firing activity when coding for a single light bar moving across the visual field, but decouple into two distinct synchronous assemblies when coding for two independent light bars (Engel, Konig, & Singer, 1991). There is evidence that coding of this type is supported by activity within the gamma (~30 – 90 Hz) frequency band (Tallon-Baudry & Bertrand, 1999; Woelbern, Eckhorn, Frien, & Bauer, 2002). Gamma activity in particular has been studied in both animals (Fries, Roelfsema, Engel, Konig, & Singer, 1997; Gail, et al., 2000; Logothetis, Pauls, Augath, Trinath, & Oeltermann, 2001; Rols, Tallon-Baudry, Girard, Bertrand, & Bullier, 2001; Siegel & Konig, 2003) and humans (Keil, Muller, Ray, Gruber, & Elbert, 1999; Tallon-Baudry, 2003), and may play a defining role in feature integration (Gray & McCormick, 1996), object recognition (Tallon-Baudry & Bertrand, 1999) and selective attention (Fell, Fernandez, Klaver, Elger, & Fries, 2003).

Numerous studies have suggested that alpha rhythms (8 – 13 Hz) may also play a key role in object processing and visual attention (Thut, Nietzel, Brandt, & Pascual-Leone, 2006; Vanni, Revonsuo, Saarinen, & Hari, 1996; Worden, Foxe, Wang, & Simpson, 2000; Yamagishi, Callan, Anderson, & Kawato, 2008; Yamagishi, et al., 2003; Yamagishi, Goda, Callan, Anderson, & Kawato, 2005). Beta rhythms (13 – 30 Hz) may be important for visuo-motor processing, including both real (Maratos, Anderson, Hillebrand, Singh, & Barnes, 2007) and imagined (Neuper, Scherer, Wriessnegger, & Pfurtscheller, 2009) interactions with objects. Recent evidence also provides strong support for the role of beta rhythms in modulating general visual attention (Kinsey, et al., 2009; Maratos, et al., 2007).

1.2 Challenges to the binding-by-synchronization hypothesis

Despite much speculation on the importance of neural oscillatory synchrony for primate vision, several reports question the functional significance of brain rhythms at any level of processing (for a review, see Shadlen & Movshon, 1999). There are specific reports, based on animal studies, that synchronized firing in a pair of neurons is not related to feature binding (Dong, Mihalas, Qiu, von der Heydt, & Niebur, 2008) or the perceptual

organization of a scene (Lamme & Spekreijse, 1998). Others suggest that synchronized activity may be minimal or absent altogether for processes related to both figure-ground patterns (Craft, Schutze, Niebur, & von der Heydt, 2007) and drifting coherent plaid patterns (Thiele & Stoner, 2003). Finally, an electroencephalographic study on humans demonstrated that the striking perceptual differences between Gestalt and non-Gestalt images were not accompanied by marked changes in gamma activity (Heinrich, Aertsen, & Bach, 2002). The failure in several studies to find changes in oscillatory activity to figure-ground patterns calls into question the specific role played by oscillatory activity in segregation and challenges the basis of the binding-by-synchronization hypothesis.

1.3 The current study

Our aim was to assess the viability of the binding-by-synchronization hypothesis and in particular characterize the role gamma rhythms may play in segregating visual objects from their background. We also sought to clarify further the role of low frequency (alpha, beta) rhythms in object processing.

In earlier MEG work, we showed that gamma activity is modulated by low-level visual features such as contrast and spatial frequency (Adjamian, Holliday, et al., 2004; Hall, et al., 2005), and is maximal for high contrast gratings of 3 c/deg periodicity (Hadjipapas, Adjamian, Swettenham, Holliday, & Barnes, 2007; Logothetis, et al., 2001). Recent evidence shows that concentric gratings also induce strong gamma activity in the early visual cortex (Hoogenboom, Schoffelen, Oostenveld, Parkes, & Fries, 2006). A wide range of stimuli yield power changes in alpha and beta within early visual cortex, including grating patterns (Maratos et al., 2007). We utilized all these findings in designing our target and background visual stimuli. Using MEG and functional magnetic resonance imaging (fMRI) retinotopic mapping, we reliably identified visual areas associated with rhythmic activity (alpha, beta and gamma) in the ventral cortex at the border of areas V1 and V2, and based our analyses on virtual electrodes at this position.

2. Method

2.1. Participants

Twelve participants (six male and six female, aged 25 – 40 years) with no history of neurological or psychiatric disorders were recruited. All participants had normal or corrected-to-normal vision. The study was undertaken with the understanding and written

consent of each subject, received local ethical committee approval and conformed to the Code of Ethics of the World Medical Association (Declaration of Helsinki).

2.2. Procedure and stimuli

All stimuli were displayed on a Dell LCD monitor at a frame rate of 60 Hz, with a resolution of 1024 lines by 768 pixels, using Presentation software (http://www.neurobs.com/) that also delivered coded stimulus identification and synchronization pulses to the MEG recording equipment.

Both non-patterned and patterned background stimuli were used. The non-patterned background consisted of a uniform blank (black) screen. The patterned background consisted of an achromatic circular square-wave grating of 3 c/deg periodicity and 95% contrast, confined within a hard-edged circular window of 12.5 deg viewing angle. The concentric rings of the background pattern were centred on the fixation point. The target stimulus (i.e. object or figure) was a circular sub-section of the background pattern, and subtended 5.5 deg of viewing angle. The centre of the target patch was presented 3.125 deg either to the left or right of fixation. Note that the target was distinguishable from the patterned background only when rotated about its own centre. Figure 1 shows examples of the stimuli as they appeared in the experiment, plus stimulus icons that are used in this paper to guide understanding of the results.

A central fixation point remained on-screen throughout the experiment, and participants were instructed to maintain fixation throughout each trial. The stimulus presentation sequence on each trial, depicted in Fig. 1 using icons, was as follows: (a) the target patch was presented to the right (left) of fixation for two seconds, initially rotating anticlockwise about its centre at 20 deg/sec for one second, then clockwise for one second, returning to its original position; (b) the screen was blank for two seconds; (c) the patterned background, centred on the fixation point, was presented for two seconds; (d) the target patch appeared to the right (left) of fixation against the patterned background for two seconds, following the same rotational movement sequence as in the initial two second period of the trial – note that a circular contour was visible throughout the target's rotation sequence but that in its original and final position the target was indistinguishable from the background; (e) the patterned background was visible for a further two seconds following the disappearance of the target patch. The inter-trial interval was 2 seconds, during which time the screen was blank except for the fixation target. This stimulus presentation cycle

was repeated 120 times, alternating between left- and right-lateralized target presentations.

Figure 1 near here

2.3. MEG co-registration, recording and pre-processing

Continuous MEG data were acquired using a 275-channel whole-head MEG system (from VSM MedTech Ltd, Port Coquitlam, BC, Canada). The sampling rate was 1200 Hz. The data were baseline-corrected and an anti-aliasing filter with a cut-off of 200 Hz was used. Third-order gradiometers and a low-pass filter of 100 Hz were applied, and notch filters (width 2 Hz) at both 50 Hz and 60 Hz were used to remove any signal artefacts arising from power lines and the display monitor. Participants sat upright in a magnetically shielded room and viewed the display monitor (located outside the room) in a front-silvered mirror (located within the room) through a small window in the room. The optical viewing distance was 2.1 m. Participants wore a headband with three electromagnetic coils attached to it. Following data acquisition, a Polhemus Isotrak 3D digitizer was used to map the surface shape of each participant's head and localise the head coils with respect to that surface. This surface was matched to the head shape extracted from MRI scans of each participant (see Adjamian, Barnes, et al., 2004 for details), enabling co-registration of MEG and MRI data to form a functional brain image.

2.4. Synthetic aperture magnetometry (SAM) 'virtual electrodes' (VEs)

A spatial filtering ('beamformer') technique known as synthetic aperture magnetometry (SAM) (Hall, et al., 2005; Hillebrand & Barnes, 2005; Hillebrand, Singh, Holliday, Furlong, & Barnes, 2005; Kinsey, et al., 2009; Robinson & J, 1999; Singh, Barnes, Hillebrand, Forde, & Williams, 2002; Van Veen, van Drongelen, Yuchtman, & Suzuki, 1997) was used to generate statistical parametric maps (SPMs) of stimulus or event-related changes in signal power (Pfurtscheller & Lopes da Silva, 1999). In brief, SAM is based on a constrained minimum-variance beamformer that allows for localized time series reconstruction of multiple uncorrelated induced signal sources in the brain. An optimal spatial filter for the 30-90 Hz frequency band – nominally the gamma band – over 'active' (post-stimulus from zero to 1.5 s) and 'passive' (pre-stimulus from -1.5 s to zero) time windows was calculated from the lead field (Sarvas, 1987) and data covariance matrix

(Van Veen, et al., 1997). The output of the beamformer is an estimate of the neuronal activity at each computed location and is referred to as the "virtual electrode" (VE), assessed using a pseudo-*t* statistic (Robinson & J, 1999). In our analysis, beamformer estimates were calculated throughout the brain volume on a 5x5x5 mm grid of points. This output was co-registered with each individual's MRI and then into standard MNI space using SPM99 (http://www.fil.ion.ucl.ac.uk/spm/snpm/).

SAM beamformer estimates for comparisons within the 30-90 Hz frequency range were made between the baseline condition (fixation only) and the target condition for both left and right visual field locations of the target patch. The results of this analysis (Fig. 2) show focal increases in gamma at the occipital poles in contralateral hemispheres. The locations of peak gamma activation in each hemisphere were chosen for subsequent time-frequency analysis (see Table 1), and participants were excluded from further analyses if activations in *each* hemisphere did not reach a pre-specified *t*-value of 3.0 (which approximates a p-value of 0.001). The time course of oscillatory power changes within both the left- and right-hemisphere VEs for each participant and for each condition was examined using a Morlet-wavelet time-frequency analysis. The spectrograms were computed using a scale of seven cycles per wavelet. This scale gives a satisfactory balance between time and frequency resolutions, and is typically used in MEG analyses using Morlet wavelet decomposition (Gruber, Maess, Trujillo-Barreto, & Muller, 2008). The resulting spectrograms were averaged across participants to create group-averaged spectrograms for each hemisphere and for each experimental condition. Note that visual inspection of the single-trial data in sensor space did not identify signal artefacts in the recordings, and no epochs were removed for further analysis in source space. Note also that the SAM beamformer actively suppresses any undetected noise or artefact sources that may have occurred in spatially removed locations, such as the eyes. This is so because the lead field patterns typically generated at the target source (occipital) are uncorrelated with those generated at the noise source (ocular) (for further discussion on SAM suppression and orthogonal lead field relationships between sources, see Brookes, et al., 2008; Brookes, et al., 2009). However, further indication that activity in the occipital VEs did not include noise contamination from the eyes was evident in that SAM images did not show significant patterns of ocular activity in the 30-90 Hz frequency band across trials (Bardouille, Picton, & Ross, 2006).

Both induced and evoked activity was assessed. Evoked activity is tightly phase-locked to the stimulus whereas induced activity is not. To reveal the level of induced (plus evoked) activity, spectrograms were created from single-trial activation waveforms for a given VE and from these an average time–frequency spectrogram was created. To demarcate evoked activity, time–frequency spectrograms were created from the average of the activation waveforms for each VE. The induced spectrograms show percentage change in energy per time–frequency bin relative to the pre-stimulus interval (T = -2 s to zero). The evoked spectrograms show amplitude change per time–frequency bin relative to the baseline (computed over T = -2 s to zero). Statistical significance of the changes was assessed using bootstrap analysis (Graimann, Huggins, Levine, & Pfurtscheller, 2002) and only changes that were significant at $p < 0.05$ are displayed in the results (see Fig. 5).

The statistical significance of the spectrogram results was assessed across participants by first setting the value of each time-frequency point where $p < 0.05$ to $p = 0.05$, yielding a conservative binary statistical significance time-frequency map for each participant. The combined p-value for each time-frequency point across participants was then calculated as

$$k \sum_{i=0}^{n-1} \frac{(-\ln(k))^i}{i!} \qquad \text{Eq. 1}$$

where n is the number of probability values to be combined (n = 7) and k = P1 * P2....*Pn is the product of the individual probabilities at each time-frequency point. Equation 1 is the n-dimensional extension of Fisher's test (Fisher, 1932), provided by l. Jost (http://www.loujost.com/Statistics%20and%20Physics/Significance%20Levels/CombiningPValues.htm). Calculated p-values were set equal to 1.0 if $p > 0.001$, and the resulting statistical significance map is given in Fig. 6, showing all time-frequency points with significant activation ($p < 0.001$) at the group level.

2.5 FMRI retinotopic mapping

To aid identification of functional MEG sources in the brain, functional boundaries within the early visual cortex were identified using the retinotopic mapping paradigm of Sereno et al. (1995). The functional magnetic resonance imaging (fMRI) scans were acquired with a

3T MR scanner (from Magnetom Trio, Siemens, Erlangen, Germany) using a gradient-echo, echo-planar (EPI) sequence (slices = 44; TR = 3000 ms; TE = 30 ms; flip angle = 90 deg; voxel size = 2.5 x 2.5 x 2.5 mm). High-resolution (1 x 1 x 1 mm) anatomical scans (MP-RAGE, Siemens) were obtained for MEG data co-registration and statistical parametric mapping. Cortical surface reconstruction and retinotopic mapping analyses were completed using the Freesurfer analysis software (http://surfer.nmr.mgh.harvard.edu/fswiki/Home). Data from the eccentricity and polar angle scans were combined to generate maps that show visual regions coded for successive mirror image and non-mirror image representations of the retinotopic projections anticipated anatomically. Visual areas V1 and V2 were identified as described in previous studies (Tootell, et al., 1997).

3. Results

3.1. Cortical localization of gamma activity

Figure 2 shows the borders of the primary and secondary visual areas on flattened cortical maps, as identified in a single participant (P1) using a standard fMRI retinotopic mapping procedure (Sereno et al., 1995). Overlaid in red are the areas where maximal gamma band activity (30 – 90 Hz) was detected (pseudo-t > 3.0) using SAM from MEG responses to the target (figure) patches presented against a blank background in either the left or right visual field (i.e. from the initial two second period of each trial; see Fig. 1). Corresponding sites of gamma activity between the flattened maps and axial brain slices are indicated by arrows. Note that hemifield stimulation resulted in significant (pseudo-t > 3.0) contralateral gamma activity within the ventral cortex at the V1/V2 border in seven participants. Table 1 shows the MNI co-ordinates of peak gamma activity (t > 3.0) for each of these participants. MEG activity in subsequent figures is estimated for these locations.

Figure 2 and Table 1 near here

3.2. Cortical dynamics during figure-ground segregation

Figure 3 shows the group-averaged (n = 7) time course of oscillatory power changes, within four separate frequency bands, for a VE placed at the site where maximal gamma

activity was recorded in each participant for each cortical hemisphere (from Fig. 2 and Table 1). Mean response power (rms Am/Hz) is plotted as a function of time (s), with the different periods of the trial demarcated by vertical dotted lines. The icons at the top of the figure indicate the presence (absence) and spatial arrangement of the target and background for each period (see also Fig. 1). The red (black) traces show the responses obtained with the target positioned in the left (right) visual field, contralateral (ipsilateral) to the VE. The blue (green) traces show the responses obtained with the target positioned in the right (left) visual field, contralateral (ipsilateral) to the VE. Details are reported below for each frequency band.

Figure 3 near here

3.2.1 High gamma frequency band (> 55 Hz)

Target presentation against a blank background (at T = 0 s) resulted in a rapid contralateral power increase in high frequency gamma, sustained until the target's disappearance at T = 2 s (red/blue traces). Ipsilateral target presentation had little effect on high gamma during this time period (black/green traces). Disappearance of the target at T = 2 s resulted in a sustained reduction in gamma. From T = 2 – 4 s, where only the fixation target was visible, the magnitude of gamma power was the same in each hemisphere. Presentation of the centrally-viewed background grating at T = 4 s resulted in another rapid rise in gamma within both hemispheres. Although not evident in Fig. 3, during the critical period of the trial from T = 6 – 8 s, when the target was presented against a patterned background, high frequency gamma activity for contralateral targets exceeded that for ipsilateral targets (between approx. 6.25 s and 7.0 s). This effect can be seen in the significance maps of Fig. 4 (discussed below).

3.2.2 Low Gamma frequency band (40 – 55 Hz)

The pattern of results for low gamma band activity was broadly similar to that for high gamma activity. The notable exception was during the critical period from T = 6 – 8 s, when the target was presented against a patterned background. Between approximately 6.25 – 7.0 s, low frequency gamma activity for contralateral targets (red/blue traces) was

less than that for ipsilateral targets (black/green traces). This is also evident in Fig. 4 (discussed below).

3.2.3 Beta frequency band (13 – 30 Hz)

Unlike the sustained change in gamma activity to the appearance of the target in isolation at T = 0 s, or its disappearance at T = 2 s, power changes within the beta band were more transitory in nature. Also unlike the results reported above for gamma, beta activity within the initial two periods of each trial was independent of the spatial location of the target; i.e. both contra- and ipsilateral targets yielded indistinguishable power changes within each hemisphere from T = 0 – 4 s. The appearance of the background at T = 4 s also produced indistinguishable contra- and ipsilateral responses. During the critical trial period from T = 6 – 8 s, when the target was presented against the patterned background, both contra- and ipsilateral stimulation yielded a decrease in beta at about 6.5 s, though the reduction tended to be greatest for contralateral stimulation (red/blue traces). The latter was more evident for the left hemisphere VE than for the right hemisphere VE.

3.2.4 Alpha frequency band (8 – 13 Hz)

The pattern of changes in alpha band activity was qualitatively similar to that reported above for beta activity across each trial period.

Figure 4 shows, for each cortical hemisphere, a group-averaged (n = 7) significance map (Mann-Whitney-Wilcoxon test, $p < 0.05$, corrected significance) of the differences between the time-frequency responses for contra- and ipsilateral targets during the ‘figure-ground’ trial period from T = 6 – 8 s: red (blue) indicates a relative increase (decrease) in power for contralateral targets. The location of the VE within each hemisphere is shown on the axial brain slice at the top of each panel (see also Fig. 2, Table 1). Each map therefore shows significant power differences between the responses obtained for the ‘figure-ground’ stimulus versus the background pattern alone. Three main effects were observed: (i) in each cortical hemisphere there was a relative increase in high-gamma power, beginning shortly after the onset of the target (across 6.25 – 6.75 s in the right hemisphere, Box a; and across 6.25 – 7.0 s in the left hemisphere, Box b); (ii) in each hemisphere there was a relative decrease in low-gamma power from approximately 6.2 – 6.9 s (Box c, Box d); and (iii) in the left cortical hemisphere there was a relative decrease in both alpha and beta power centred at approximately T = 6.5 s (Box e). Note that the increase in gamma associated with the onset of the target against a blank background persisted for nearly 2 s

(see Fig. 3, T = 0 – 2 s), whereas the relative changes in gamma associated with the onset of the target against a patterned background lasted 0.5 – 0.75 s.

Figure 4 near here

3.3 Evoked versus induced responses

Figure 5 shows the time–frequency plots for activity at the V1/V2 border in the left hemisphere (from Fig. 2) for a single representative participant, depicting both evoked activity (top panels) and induced-plus-evoked activity (bottom panels). The time axis is partitioned into the five components of the stimulus presentation cycle, as indicated by the icons at the top of the figure. The red/blue colour scales represent significant ($p < 0.05$) changes in amplitude (evoked spectrograms) or energy (induced-plus-evoked spectrograms). Note that evoked activity was confined to the alpha/beta frequency range and was transient in nature. It was most evident shortly after the onset of the target in isolation (at T = 0 s, Box a), at the offset of the target (at T = 2 s, Box b), and again shortly after the onset of the background pattern (at T = 4 s, Box c). At the onset of the figure (T = 6 s), there is evidence of a small amount of evoked activity confined to the alpha frequency region (Box d). Note, however, there is no evoked activity at the time of motion reversal (T = 7 s, Box e). The spectral power changes evident within the gamma frequency range in the induced-plus-evoked spectrograms (Box f) were not reflected in the evoked spectrograms (Box g). This same pattern of results is reflected in the group-averaged (n = 7) significance maps ($p < 0.01$) of power changes (see Fig. 6). This indicates that the gamma activity we observed in this study must reflect induced activity, which is consistent with previous studies (Adjamian, Holliday, et al., 2004; Hadjipapas, et al., 2007; Hall, et al., 2005; Muthukumaraswamy, Singh, Swettenham, & Jones, 2009).

Figures 5 and 6 near here

From Figs. 5 and 6, note also that there is a marked decrease in alpha/beta activity shortly after the start of each time frame (i.e. near 0.5 s, 2.5 s, and 4.5 s), consistent with the fluctuations evident in alpha/beta power shown in the group data of Fig. 3.

4. Discussion

Our goal was to characterise the role brain rhythms may play in object processing and in segregating an object from its background. Using MEG we identified a region within each hemisphere at the border of areas V1 and V2 where robust oscillatory activity was evident during the perception of a grating patch (our target object). Data analyses using synthetic aperture magnetometry were conducted for a virtual electrode placed at this location.

MEG responses to the target stimulus varied depending on whether it was presented against a uniform or patterned background. When the target was presented against a uniform background, striking differences were apparent between the response profiles for low- (alpha and beta) and high-frequency (gamma) activity. We observed sustained power changes in gamma but transitory power changes in alpha and beta (see Fig. 3 for the trial period T = 0 – 2 s). Further, the changes in gamma were only evident within the contralateral hemisphere, whereas the power changes in alpha and beta were evident within both contralateral and ipsilateral hemispheres (Fig. 3, T = 0 – 2 s). The dependence of gamma on the spatial location of the target provides support for its putative role in visual object coding (e.g. Adjamian et al., 2004; Hall et al., 2005). However, because the power changes in alpha and beta were independent of target location, we conclude that their presence may signify a more general role in object processing, perhaps related to attentional mechanisms (see also Maratos et al., 2007).

Assessment of the MEG responses to target stimuli presented against a patterned background were analyzed to determine the role of cortical oscillations in ‘figure-ground’ processing. These results relate to the critical trial period from T = 6 – 8 s (see Figs. 3 - 6), and are discussed below for both high- and low-frequency oscillatory activity.

4.1 High frequency activity (> 40 Hz)

Appearance of the target against a patterned background yielded, within the same brain volume, an increase in high-gamma (> 55 Hz) power accompanied by a decrease in low-gamma (40-55 Hz) power (Figs. 3 and 4). These changes reflected non-phased locked

activity (Figs. 5, 6). Such changes could be consequent upon a shift in gamma to a range of higher frequencies, a phenomenon that has been noted to occur immediately following the onset of grating patterns (Hall et al., 2005). However, in this study we found no evidence for an upward shift of the gamma frequency range following the onset of our target patch (see Fig. 5, panel T = 6 – 8 s).

The role of gamma rhythms in figure-ground segregation is hypothesised to result from one or two general processes: (i) region labelling, achieved by labelling corresponding elements in an isomorphic surface representation (Lamme, 1995); and/or (ii) border ownership coding, achieved through contour representation following the activity of orientation-selective units (Craft, et al., 2007). These different schemes may explain the opposing power changes in gamma reported here. While opposing power changes in gamma within the same visual area have not been reported before, we note that previous studies on figure-ground segregation have reported either increases (Lamme, 1995; Zipser, Lamme, & Schiller, 1996) or decreases (Gail et al., 2000) in gamma activity. Evidence from previous experimental work, together with theoretical arguments on the nature of brain rhythms, suggest that increases in gamma may relate to the process of region labelling whereas decreases in gamma may relate to the process of border ownership. For example, studies on figure-ground coding in monkey V1 have reported enhanced spike rates within an object's surface representation (Lamme, 1995; Zipser, et al., 1996). On the other hand, multi-unit cellular recording in non-human primates showed strong decoupling of population activity across a figure/ground border (Gail, et al., 2000). The latter is supported by Eckhorn et als. (2004) model, where power decreases in gamma observed in figure-background segregation stem from orientation-defined contours disrupting lateral coupling connections between neurons. Thus, segregation of the figure and background stimuli may depend on the coding of border ownership (Craft, et al., 2007).

Power increases in high frequency gamma may also represent attentional changes in response to global motion onset. In a recent study examining motion processing and oscillatory activity (Swettenham, Muthukumaraswamy, & Singh, 2009), significant power increases in high frequency gamma were reported for moving gratings, while changes in low frequency gamma were associated with static stimuli. Similarly, Siegel et al. (2007) concluded from their data that high frequency gamma (60-100 Hz) was specific for coding visual motion signals. Given these findings, we cannot exclude the possibility that the

power increases in high frequency gamma we observed may represent specific coding for the motion component of the figure (i.e. the figure's slow rotation clockwise/anticlockwise – see Methods). However, we note that no increase in gamma was evident on reversal of the figure's rotational motion at T = 7 s (Fig. 4), where the motion transient was greatest.

Modulation of cortical oscillations within a brain region can either be stimulus driven or in response to feedback from higher-order cortical areas. While some have argued that feature segmentation and grouping occurs automatically and pre-attentively (Scholte, Witteveen, Spekreijse, & Lamme, 2006), other have shown that gamma activity is strongly identified with attentional mechanisms (Halgren, et al., 2003; Herrmann & Mecklinger, 2000; Kaiser, Buhler, & Lutzenberger, 2004; Vidal, Chaumon, O'Regan, & Tallon-Baudry, 2006). One hypothesis is that top-down effects support segregation and grouping of visual features. For example, lesions in the dorsal extra-striate area (Super & Lamme, 2007) and anaesthesia (Lamme, Zipser, & Spekreijse, 1998) can reduce the figure-ground effect. Moreover, functional imaging studies suggest that higher visual areas such as V4 may contribute to texture segmentation as well as illusory contour detection (Kastner & Ungerleider, 2001; Mendola, Dale, Fischl, Liu, & Tootell, 1999). As suggested by Qiu, Sugihara and von der Heydt (2007), such attentional mechanisms associated with figure-ground segregation are independent of border ownership coding but interact with signal neurons in area V2. From our data (Fig. 4), the late occurrence of gamma changes (~250 ms after target onset) in the V1/V2 region supports the notion that feedback from higher cortical areas is important for figure-ground segregation.

4.2 Low frequency activity (< 40 Hz)

The origin of low frequency rhythms and their role in information processing both within and between brain areas continue to be debated. Historically, the alpha rhythm (8 – 13 Hz) has received the most interest. The standard view is that large-amplitude alpha characterizes an idling cortical network (Adrian & Matthews, 1934; Pfurtscheller, 2001; Pfurtscheller, Stancak, & Neuper, 1996). However, some studies provide evidence for task-dependent increases in alpha (Jensen, Gelfand, Kounios, & Lisman, 2002; Klimesch, 1999; Worden, et al., 2000). In a series of studies, Yamagishi et al. (2008; 2003; 2005) suggested that increased alpha in the calcarine may serve to enhance the efficiency of processing information related to the visual stimulus, and that power changes in alpha (both increases and decreases) may be an integral part of the neuronal operations associated with engaging, disengaging and shifting attention. Various other studies

provide evidence that power changes in alpha may also be important for controlling interactions between brain regions (also see Hummel, Andres, Altenmuller, Dichgans, & Gerloff, 2002; Mima, Oluwatimilehin, Hiraoka, & Hallett, 2001; Pfurtscheller & Lopes da Silva, 1999; Sauseng, et al., 2005; Thut, et al., 2006; Worden, et al., 2000; Yamagishi, et al., 2005).

The functional role of low frequency oscillatory activity in figure-background segregation has largely been unexplored. In our study, we observed that, unlike the sustained changes in gamma to the appearance and disappearance of stimuli, power changes within alpha and beta were of a transitory nature (Figs. 3 & 4). These results are broadly consistent with Van der Togt's (2006) EEG study, which showed that enhanced low frequency activity (< 20 Hz) prior to stimulus onset was followed by a decrease in activity post-stimulus onset, results that were interpreted within the context of attentional modulations. Indeed, previous work has demonstrated a link between gamma binding and attentional mechanisms linked to activity within the alpha frequency band (Ward, 2003).

Perhaps the most striking difference we observed between high- (gamma) and low-frequency (alpha/beta) activity was the dependence or not on the spatial location of the target. Unlike the results for gamma, power changes in alpha and beta were independent of the spatial location of the target when it was presented against a blank background (compare gamma activity with alpha/beta activity in Fig. 3 for T = 0 – 2 s). And again during the critical trial period, when the target was presented against a patterned background, both contralateral and ipsilateral stimulation yielded reductions in alpha and beta (see Fig. 3 for T ~ 6.5 s). Although the reduction in alpha/beta was greatest for contralateral stimulation, the difference only reached significance for the left hemisphere (Fig. 4). It should be noted however that the amplitude of the alpha/beta responses reported here may be sub-optimal as the low frequency activity was estimated for a location of interest defined by peak gamma activity (namely at the V1/V2 border). This was unavoidable if we were to satisfy our aim of comparing response profiles of different oscillatory rhythms within the same brain area. Nonetheless, we note that our amplitude measures for alpha/beta are similar to those reported using VEs optimally positioned for low frequency activity (Maratos et al., 2007).

In summary, although the changes in gamma activity at the V1/V2 border appear directly related to processing visual targets, the changes in alpha and beta activity do not. While

not discounting a possible role in figure-ground segregation, we concur with other studies that the principal role of alpha and beta rhythms in object processing may relate more to changes in visual attention. The role of gamma, on the other hand, is much more tightly bound to the figural properties of the visual stimulus. Notably, gamma is modulated by the emergence of the figure against the patterned background, when presumably large numbers of neurones are already strongly activated by the background itself. The spatial frequency and contrast of the target are equal to the background and consequently the gamma modulation we observed cannot be a consequence of gross changes in the incoming sensory projection to the cortex, as might be the case when the target appears in isolation (i.e. against a uniform background). Therefore, we assume our results reflect processing of figural information within the cortex, at a stage following the initial projection of information from the LGN. This conclusion is supported by our results showing an absence of evoked gamma activity linked to the onset of the figure (Fig. 5, Box g at T = 6 s; Fig. 6), as evoked activity is often linked to this early stage processing.

References

Adjamian, P., Barnes, G. R., Hillebrand, A., Holliday, I. E., Singh, K. D., Furlong, P. L., et al. (2004). Co-registration of magnetoencephalography with magnetic resonance imaging using bite-bar-based fiducials and surface-matching. *Clin Neurophysiol, 115*(3), 691-698.

Adjamian, P., Holliday, I. E., Barnes, G. R., Hillebrand, A., Hadjipapas, A., & Singh, K. D. (2004). Induced visual illusions and gamma oscillations in human primary visual cortex. *Eur J Neurosci, 20*(2), 587-592.

Adrian, E. D., & Matthews, B. H. C. (1934). The Berger rhythm: potential changes from the occipital lobes in man. *Brain, 57*(355).

Bardouille, T., Picton, T. W., & Ross, B. (2006). Correlates of eye blinking as determined by synthetic aperture magnetometry. *Clin Neurophysiol, 117*(5), 952-958.

Brookes, M. J., Stevenson, C. M., Hadgipapas, A., Barnes, G. R., Mullinger, K. J., Bagshaw, A. P., et al. (2008). Beamformer Imaging and Interference Rejection. In R. Kakigi, K. Yokosawa & S. Kuriki (Eds.), *Boimagnetism. Interdisiplinary research and exploration* (pp. 62-64): Hokkaido University Press.

Brookes, M. J., Vrba, J., Mullinger, K. J., Geirsdottir, G. B., Yan, W. X., Stevenson, C. M., et al. (2009). Source localisation in concurrent EEG/fMRI: applications at 7T. *Neuroimage, 45*(2), 440-452.

Bullier, J. (2001). Integrated model of visual processing. *Brain Res Brain Res Rev, 36*(2-3), 96-107.

Craft, E., Schutze, H., Niebur, E., & von der Heydt, R. (2007). A neural model of figure-ground organization. *J Neurophysiol, 97*(6), 4310-4326.

Crick, F. (1994). *The Astonishing Hypothesis*. London: Simon and Schuster.

Dong, Y., Mihalas, S., Qiu, F., von der Heydt, R., & Niebur, E. (2008). Synchrony and the binding problem in macaque visual cortex. *J Vis, 8*(7), 30 31-16.

Eckhorn, R., Bauer, R., Jordan, W., Brosch, M., Kruse, W., Munk, M., et al. (1988). Coherent oscillations: a mechanism of feature linking in the visual cortex? Multiple electrode and correlation analyses in the cat. *Biol Cybern, 60*(2), 121-130.

Eckhorn, R., Gail, A., Bruns, A., Gabriel, A., Al-Shaikhli, B., & Saam, M. (2004). Neural mechanisms of visual associative processing. *Acta Neurobiol Exp (Wars), 64*(2), 239-252.

Engel, A. K., Konig, P., & Singer, W. (1991). Direct physiological evidence for scene segmentation by temporal coding. *Proc Natl Acad Sci U S A, 88*(20), 9136-9140.

Fell, J., Fernandez, G., Klaver, P., Elger, C. E., & Fries, P. (2003). Is synchronized neuronal gamma activity relevant for selective attention? *Brain Res Brain Res Rev, 42*(3), 265-272.

Fisher, R. A. (1932). *Statistical Methods for Research Workers*. Edinburgh: Oliver and Boyd.

Fries, P., Roelfsema, P. R., Engel, A. K., Konig, P., & Singer, W. (1997). Synchronization of oscillatory responses in visual cortex correlates with perception in interocular rivalry. *Proc Natl Acad Sci U S A, 94*(23), 12699-12704.

Gail, A., Brinksmeyer, H. J., & Eckhorn, R. (2000). Contour decouples gamma activity across texture representation in monkey striate cortex. *Cereb Cortex, 10*(9), 840-850.

Graimann, B., Huggins, J. E., Levine, S. P., & Pfurtscheller, G. (2002). Visualization of significant ERD/ERS patterns in multichannel EEG and ECoG data. *Clin Neurophysiol, 113*(1), 43-47.

Gray, C. M., & McCormick, D. A. (1996). Chattering cells: superficial pyramidal neurons contributing to the generation of synchronous oscillations in the visual cortex. *Science, 274*(5284), 109-113.

Gray, C. M., & Singer, W. (1989). Stimulus-specific neuronal oscillations in orientation columns of cat visual cortex. *Proc Natl Acad Sci U S A, 86*(5), 1698-1702.

Gruber, T., Maess, B., Trujillo-Barreto, N. J., & Muller, M. M. (2008). Sources of synchronized induced Gamma-Band responses during a simple object recognition task: a replication study in human MEG. *Brain Res, 1196*, 74-84.

Hadjipapas, A., Adjamian, P., Swettenham, J. B., Holliday, I. E., & Barnes, G. R. (2007). Stimuli of varying spatial scale induce gamma activity with distinct temporal characteristics in human visual cortex. *Neuroimage, 35*(2), 518-530.

Halgren, E., Mendola, J., Chong, C. D., & Dale, A. M. (2003). Cortical activation to illusory shapes as measured with magnetoencephalography. *Neuroimage, 18*(4), 1001-1009.

Hall, S. D., Holliday, I. E., Hillebrand, A., Singh, K. D., Furlong, P. L., Hadjipapas, A., et al. (2005). The missing link: analogous human and primate cortical gamma oscillations. *Neuroimage, 26*(1), 13-17.

Heinrich, S. P., Aertsen, A., & Bach, M. (2002). Striking Gestalt modulates EEG gamma activity - but not in accordance with the temporal binding hypothesis. *Journal of Vision, 2*(7), 230a.

Herrmann, C. S., & Mecklinger, A. (2000). Magnetoencephalographic responses to illusory figures: early evoked gamma is affected by processing of stimulus features. *Int J Psychophysiol, 38*(3), 265-281.

Hillebrand, A., & Barnes, G. R. (2005). Beamformer analysis of MEG data. *Int Rev Neurobiol, 68*, 149-171.

Hillebrand, A., Singh, K. D., Holliday, I. E., Furlong, P. L., & Barnes, G. R. (2005). A new approach to neuroimaging with magnetoencephalography. *Hum Brain Mapp, 25*(2), 199-211.

Hoogenboom, N., Schoffelen, J. M., Oostenveld, R., Parkes, L. M., & Fries, P. (2006). Localizing human visual gamma-band activity in frequency, time and space. *Neuroimage, 29*(3), 764-773.

Hubel, D. H., & Wiesel, T. N. (1962). Receptive fields, binocular interaction and functional architecture in the cat's visual cortex. *J Physiol, 160*, 106-154.

Hubel, D. H., & Wiesel, T. N. (1968). Receptive fields and functional architecture of monkey striate cortex. *J Physiol, 195*(1), 215-243.

Hummel, F., Andres, F., Altenmuller, E., Dichgans, J., & Gerloff, C. (2002). Inhibitory control of acquired motor programmes in the human brain. *Brain, 125*(Pt 2), 404-420.

Jensen, O., Gelfand, J., Kounios, J., & Lisman, J. E. (2002). Oscillations in the alpha band (9-12 Hz) increase with memory load during retention in a short-term memory task. *Cereb Cortex, 12*(8), 877-882.

Kaiser, J., Buhler, M., & Lutzenberger, W. (2004). Magnetoencephalographic gamma-band responses to illusory triangles in humans. *Neuroimage, 23*(2), 551-560.

Kastner, S., & Ungerleider, L. G. (2001). The neural basis of biased competition in human visual cortex. *Neuropsychologia, 39*(12), 1263-1276.

Keil, A., Muller, M. M., Ray, W. J., Gruber, T., & Elbert, T. (1999). Human gamma band activity and perception of a gestalt. *J Neurosci, 19*(16), 7152-7161.

Kinsey, K., Anderson, S. J., Hadjipapas, A., Nevado, A., Hillebrand, A., & Holliday, I. E. (2009). Cortical oscillatory activity associated with the perception of illusory and real visual contours. *Int J Psychophysiol, 73*(3), 265-272.

Klimesch, W. (1999). EEG alpha and theta oscillations reflect cognitive and memory performance: a review and analysis. *Brain Res Brain Res Rev, 29*(2-3), 169-195.

Kreiter, A. K., & Singer, W. (1996). Stimulus-dependent synchronization of neuronal responses in the visual cortex of the awake macaque monkey. *J Neurosci, 16*(7), 2381-2396.

Lamme, V. A. (1995). The neurophysiology of figure-ground segregation in primary visual cortex. *J Neurosci, 15*(2), 1605-1615.

Lamme, V. A., & Spekreijse, H. (1998). Neuronal synchrony does not represent texture segregation. *Nature, 396*(6709), 362-366.

Lamme, V. A., Zipser, K., & Spekreijse, H. (1998). Figure-ground activity in primary visual cortex is suppressed by anesthesia. *Proc Natl Acad Sci U S A, 95*(6), 3263-3268.

Logothetis, N. K., Pauls, J., Augath, M., Trinath, T., & Oeltermann, A. (2001). Neurophysiological investigation of the basis of the fMRI signal. *Nature, 412*(6843), 150-157.

Maratos, F. A., Anderson, S. J., Hillebrand, A., Singh, K. D., & Barnes, G. R. (2007). The spatial distribution and temporal dynamics of brain regions activated during the perception of object and non-object patterns. *Neuroimage, 34*(1), 371-383.

Mendola, J. D., Dale, A. M., Fischl, B., Liu, A. K., & Tootell, R. B. (1999). The representation of illusory and real contours in human cortical visual areas revealed by functional magnetic resonance imaging. *J Neurosci, 19*(19), 8560-8572.

Mima, T., Oluwatimilehin, T., Hiraoka, T., & Hallett, M. (2001). Transient interhemispheric neuronal synchrony correlates with object recognition. *J Neurosci, 21*(11), 3942-3948.

Muthukumaraswamy, S. D., Singh, K. D., Swettenham, J. B., & Jones, D. K. (2009). Visual gamma oscillations and evoked responses: variability, repeatability and structural MRI correlates. *Neuroimage, 49*(4), 3349-3357.

Neuper, C., Scherer, R., Wriessnegger, S., & Pfurtscheller, G. (2009). Motor imagery and action observation: modulation of sensorimotor brain rhythms during mental control of a brain-computer interface. *Clin Neurophysiol, 120*(2), 239-247.

Pfurtscheller, G. (2001). Functional brain imaging based on ERD/ERS. *Vision Res, 41*(10-11), 1257-1260.

Pfurtscheller, G., & Lopes da Silva, F. H. (1999). Event-related EEG/MEG synchronization and desynchronization: basic principles. *Clin Neurophysiol, 110*(11), 1842-1857.

Pfurtscheller, G., Stancak, A., Jr., & Neuper, C. (1996). Event-related synchronization (ERS) in the alpha band--an electrophysiological correlate of cortical idling: a review. *Int J Psychophysiol, 24*(1-2), 39-46.

Qiu, F. T., Sugihara, T., & von der Heydt, R. (2007). Figure-ground mechanisms provide structure for selective attention. *Nat Neurosci, 10*(11), 1492-1499.

Robinson, S. E., & J, V. (1999). *Functional neuroimaging by synthetic aperture magnetometry (SAM)*. Sendai: Tohoku University Press.

Rols, G., Tallon-Baudry, C., Girard, P., Bertrand, O., & Bullier, J. (2001). Cortical mapping of gamma oscillations in areas V1 and V4 of the macaque monkey. *Vis Neurosci, 18*(4), 527-540.

Sarvas, J. (1987). Basic mathematical and electromagnetic concepts of the biomagnetic inverse problem. *Phys Med Biol, 32*(1), 11-22.

Sauseng, P., Klimesch, W., Stadler, W., Schabus, M., Doppelmayr, M., Hanslmayr, S., et al. (2005). A shift of visual spatial attention is selectively associated with human EEG alpha activity. *Eur J Neurosci, 22*(11), 2917-2926.

Scholte, H. S., Witteveen, S. C., Spekreijse, H., & Lamme, V. A. (2006). The influence of inattention on the neural correlates of scene segmentation. *Brain Res, 1076*(1), 106-115.

Sereno, M. I., Dale, A. M., Reppas, J. B., Kwong, K. K., Belliveau, J. W., Brady, T. J., et al. (1995). Borders of multiple visual areas in humans revealed by functional magnetic resonance imaging. *Science, 268*(5212), 889-893.

Shadlen, M. N., & Movshon, J. A. (1999). Synchrony unbound: a critical evaluation of the temporal binding hypothesis. *Neuron, 24*(1), 67-77, 111-125.

Siegel, M., Donner, T. H., Oostenveld, R., Fries, P., & Engel, A. K. (2007). High-frequency activity in human visual cortex is modulated by visual motion strength. *Cereb Cortex, 17*(3), 732-741.

Siegel, M., & Konig, P. (2003). A functional gamma-band defined by stimulus-dependent synchronization in area 18 of awake behaving cats. *J Neurosci, 23*(10), 4251-4260.

Singer, W. (1999). Neuronal synchrony: a versatile code for the definition of relations? *Neuron, 24*(1), 49-65, 111-125.

Singer, W. (2007). Binding by synchrony. *Scholarpedia, 2*(12), 1657. doi:10.4249/scholarpedia.1657

Singh, K. D., Barnes, G. R., Hillebrand, A., Forde, E. M., & Williams, A. L. (2002). Task-related changes in cortical synchronization are spatially coincident with the hemodynamic response. *Neuroimage, 16*(1), 103-114.

Super, H., & Lamme, V. A. (2007). Altered figure-ground perception in monkeys with an extra-striate lesion. *Neuropsychologia, 45*(14), 3329-3334.

Swettenham, J. B., Muthukumaraswamy, S. D., & Singh, K. D. (2009). Spectral properties of induced and evoked gamma oscillations in human early visual cortex to moving and stationary stimuli. *J Neurophysiol, 102*(2), 1241-1253.

Tallon-Baudry, C. (2003). Oscillatory synchrony and human visual cognition. *J Physiol Paris, 97*(2-3), 355-363.

Tallon-Baudry, C., & Bertrand, O. (1999). Oscillatory gamma activity in humans and its role in object representation. *Trends Cogn Sci, 3*(4), 151-162.

Thiele, A., & Stoner, G. (2003). Neuronal synchrony does not correlate with motion coherence in cortical area MT. *Nature, 421*(6921), 366-370.

Thielscher, A., Kolle, M., Neumann, H., Spitzer, M., & Gron, G. (2008). Texture segmentation in human perception: A combined modeling and fMRI study. *Neuroscience, 151*(3), 730-736.

Thut, G., Nietzel, A., Brandt, S. A., & Pascual-Leone, A. (2006). Alpha-band electroencephalographic activity over occipital cortex indexes visuospatial attention bias and predicts visual target detection. *J Neurosci, 26*(37), 9494-9502.

Tootell, R. B., Mendola, J. D., Hadjikhani, N. K., Ledden, P. J., Liu, A. K., Reppas, J. B., et al. (1997). Functional analysis of V3A and related areas in human visual cortex. *J Neurosci, 17*(18), 7060-7078.

van der Togt, C., Kalitzin, S., Spekreijse, H., Lamme, V. A., & Super, H. (2006). Synchrony dynamics in monkey V1 predict success in visual detection. *Cereb Cortex, 16*(1), 136-148.

Van Essen, D. C. (Ed.). (2004). *Organization of visual areas in macaque and human cerebral cortex* (Vol. 1): MIT Press.

Van Veen, B. D., van Drongelen, W., Yuchtman, M., & Suzuki, A. (1997). Localization of brain electrical activity via linearly constrained minimum variance spatial filtering. *IEEE Trans Biomed Eng, 44*(9), 867-880.

Vanni, S., Revonsuo, A., Saarinen, J., & Hari, R. (1996). Visual awareness of objects correlates with activity of right occipital cortex. *Neuroreport, 8*(1), 183-186.

Vidal, J. R., Chaumon, M., O'Regan, J. K., & Tallon-Baudry, C. (2006). Visual grouping and the focusing of attention induce gamma-band oscillations at different frequencies in human magnetoencephalogram signals. *J Cogn Neurosci, 18*(11), 1850-1862.

Ward, L. M. (2003). Synchronous neural oscillations and cognitive processes. *Trends Cogn Sci, 7*(12), 553-559.

Woelbern, T., Eckhorn, R., Frien, A., & Bauer, R. (2002). Perceptual grouping correlates with short synchronization in monkey prestriate cortex. *Neuroreport, 13*(15), 1881-1886.

Worden, M. S., Foxe, J. J., Wang, N., & Simpson, G. V. (2000). Anticipatory biasing of visuospatial attention indexed by retinotopically specific alpha-band electroencephalography increases over occipital cortex. *J Neurosci, 20*(6), RC63.

Yamagishi, N., Callan, D. E., Anderson, S. J., & Kawato, M. (2008). Attentional changes in pre-stimulus oscillatory activity within early visual cortex are predictive of human visual performance. *Brain Res, 1197*, 115-122.

Yamagishi, N., Callan, D. E., Goda, N., Anderson, S. J., Yoshida, Y., & Kawato, M. (2003). Attentional modulation of oscillatory activity in human visual cortex. *Neuroimage, 20*(1), 98-113.

Yamagishi, N., Goda, N., Callan, D. E., Anderson, S. J., & Kawato, M. (2005). Attentional shifts towards an expected visual target alter the level of alpha-band oscillatory activity in the human calcarine cortex. *Brain Res Cogn Brain Res, 25*(3), 799-809.

Zipser, K., Lamme, V. A., & Schiller, P. H. (1996). Contextual modulation in primary visual cortex. *J Neurosci, 16*(22), 7376-7389.

804
805
806
807
808
809
810
811
812
813
814
815

816 **Figure Captions**

817

818 Figure 1. The top panels depict the target and target-background stimuli as they appeared
819 on the experimental display screen: the bi-directional arrows signify that the target
820 was rotated about its own centre by +/- 20 deg. The bottom panels show the
821 stimulus presentation sequence on each trial, depicted using icons, from time zero
822 to ten seconds.

823

824 Figure 2. Visual areas identified in a single participant (P1, Table 2) using a standard fMRI
825 BOLD retinotopic mapping procedure: the field-sign map includes retinotopic areas
826 V1 and V2 (ventral and dorsal). Areas coloured yellow represent the visual field in
827 normal polarity, while areas coloured blue represent a mirror-reversed visual field.
828 Overlaid in red on the flattened cortical maps are the areas where peak gamma
829 activity (30 – 90 Hz) was evident in the left hemisphere (MNI = -15, -87, -9) for a
830 right lateralized target, and in the right hemisphere (MNI = 12, -90, -9) for a left
831 lateralized target (as depicted by stimulus icons at the top of the figure).
832 Corresponding sites of gamma activity between the flattened maps and axial brain
833 slices are indicated by white arrows.

834

835 Figure 3. Group-averaged (n = 7) time course of oscillatory power changes within alpha (8-
836 13 Hz), beta (15-30 Hz), low-gamma (40-55 Hz) and high-gamma (> 55 Hz)
837 frequency bands for a VE placed at the site of peak gamma activity in each cortical
838 hemisphere (from Fig. 2 and Table 1). Mean response power (rms Am/Hz) is plotted
839 as a function of time (s), with the different periods of the trial demarcated by vertical
840 dotted lines: the icons at the top of the figure indicate the presence (absence) and
841 spatial arrangement of the target and background for each period. The red (black)
842 traces show the responses obtained with the target positioned in the left (right)
843 visual field, contralateral (ipsilateral) to the position of the VE. The blue (green)
844 traces show the responses obtained with the target positioned in the right (left)
845 visual field, contralateral (ipsilateral) to the position of the VE.

846

847 Figure 4. Group-averaged (n = 7) significance map (Mann-Whitney-Wilcoxon test, $p < 0.05$, $|Z| > 1.96$) of the differences between the time-frequency responses for left-
848 and right-lateralized targets for the trial period from 6 – 8 s: red (blue) indicates a
849 *relative* increase (decrease) in power for left-lateralized targets. The results are
850

based on a VE within each cortical hemisphere, as indicated on the axial brain slices at the top of each panel (see also Fig. 2, Table 1). The colour scale shows Z scores computed from the Mann-Whitney-Wilcoxon distribution, thresholded at |Z|> 1.96. See text for explanation of Boxes a – e.

Figure 5. Morlet-wavelet time–frequency spectrograms for activity at the V1/V2 border in the left hemisphere (from Fig. 2 for participant P1), depicting both evoked activity (top panels) and induced (plus evoked) activity (bottom panels). The time axis is partitioned into the five components of the stimulus presentation cycle (see stimulus icons). The red/blue colour scales represent significant changes in amplitude (evoked spectrograms) or energy (induced-plus-evoked spectrograms). The evoked spectrograms show amplitude (fAm/Hz) change per time–frequency bin relative to baseline (computed over T = -2 s to zero). The induced spectrograms show percentage change in energy per time–frequency bin relative to the pre-stimulus interval (T = -2 s to zero). Statistical significance of the changes was assessed using bootstrap analysis, and only changes that were significant at $p < 0.05$ are displayed in the results. See text for explanation of boxes a – g.

Figure 6. Combined significance maps of power changes in cortical activity at the V1/V2 border in the left hemisphere locations given in Table 1 for all participants (n = 7). Statistically significant ($p < 0.001$) levels of evoked activity (a, top panel) and induced (plus evoked) activity (b, bottom panel) are shown for frequencies from 0 – 80 Hz as a function of time (s) from 0 – 10 s. The time axis is partitioned into the five components of the stimulus presentation cycle, as indicated by the stimulus icons at the top of the figure.

Participant	**Left Hemisphere Peak t-value** (MNI)	**Right Hemisphere Peak t-value** (MNI)
P1	**6.1** (-15, -87, -9)	**6.3** (12, -90, -9)
P2	**4.5** (-18, -81, -18)	**7.0** (6, -87, -12)
P3	**5.0** (-12, -81, -6)	**4.6** (18, -87, 3)
P4	**4.1** (-30, -75, 3)	**3.9** (4, -78, -3)
P5	**3.0** (-10, -90, -17)	**3.6** (15, -90, -6)
P6	**7.6** (-12, -84, -9)	**4.9** (9, -87, -15)
P7	**7.5** (-18, -90, -18)	**5.5** (9, -93, -18)

Table 1: MNI co-ordinates of peak voxel activity (t > 3.0) for gamma activity (30 – 90 Hz) within the ventral cortex at the V1/V2 border in seven participants, based on MEG responses to hemifield presentation of the target ('figure') patches against a blank background. Note that for each participant, hemifield stimulation resulted in significant contralateral gamma activity.

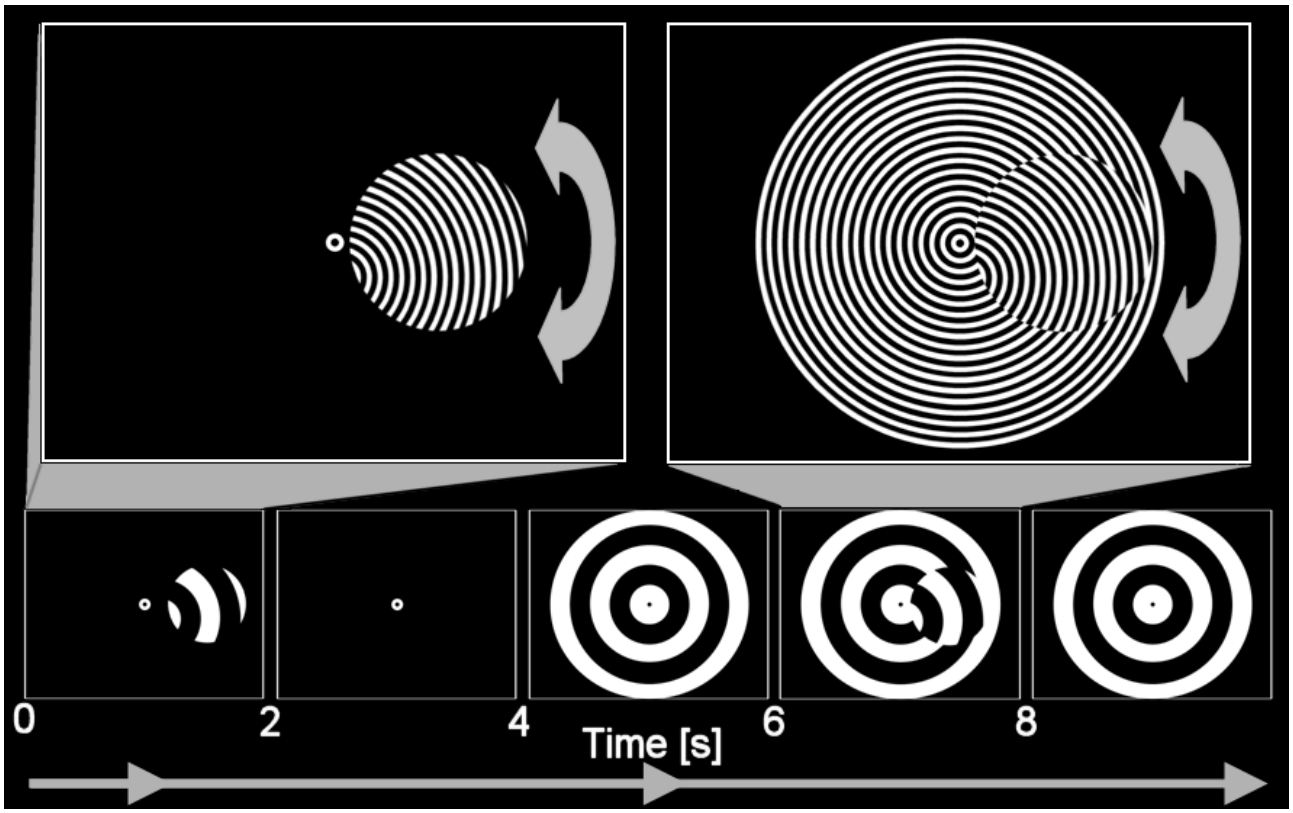

Figure 1

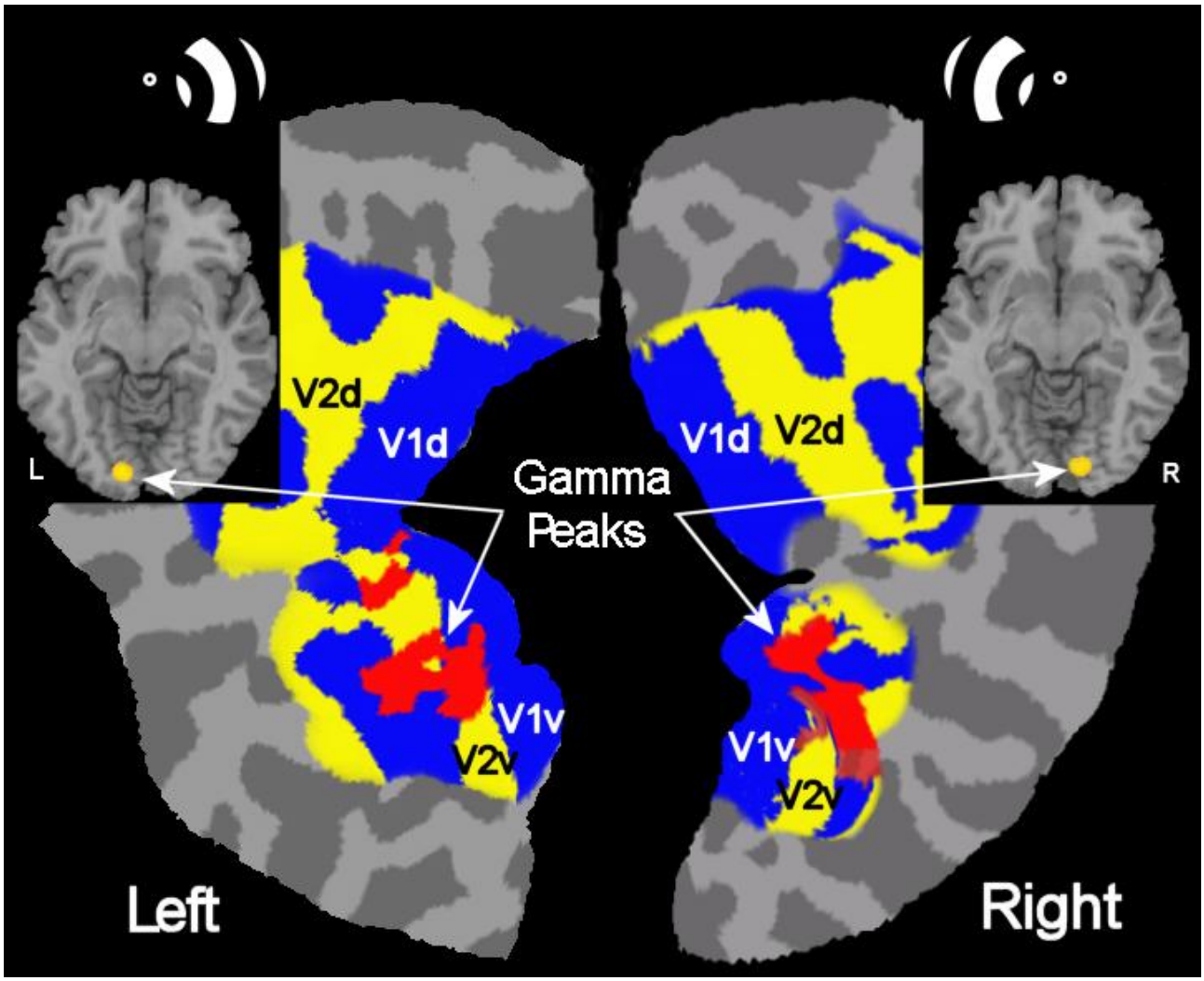

Figure 2

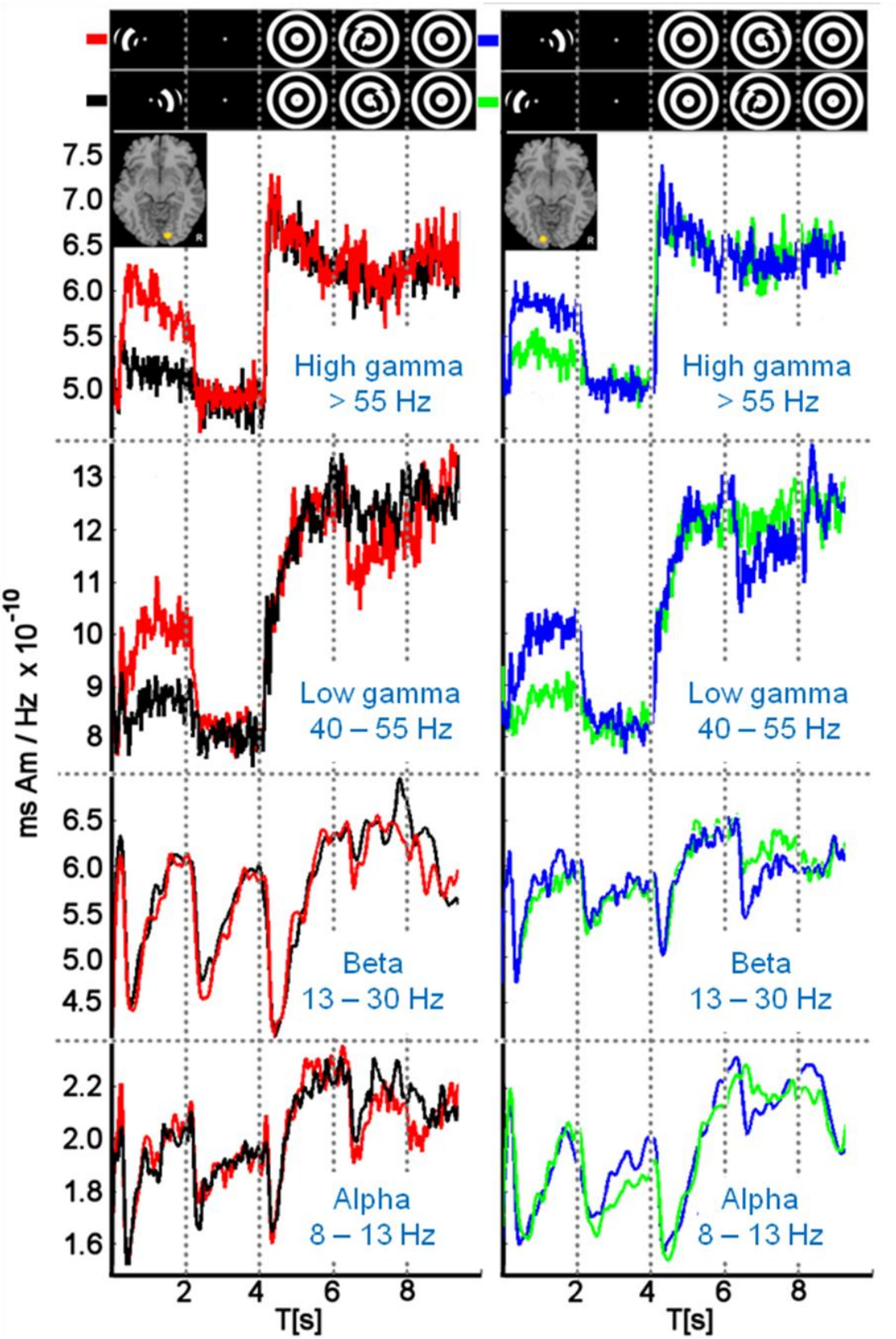
High gamma
> 55 Hz
High gamma
> 55 Hz
Low gamma
40 – 55 Hz
Low gamma
40 – 55 Hz
Beta
13 – 30 Hz
Beta
13 – 30 Hz
Alpha
8 – 13 Hz
Alpha
8 – 13 Hz
ms Am / Hz x 10^-10
T[s]
T[s]

Figure 3

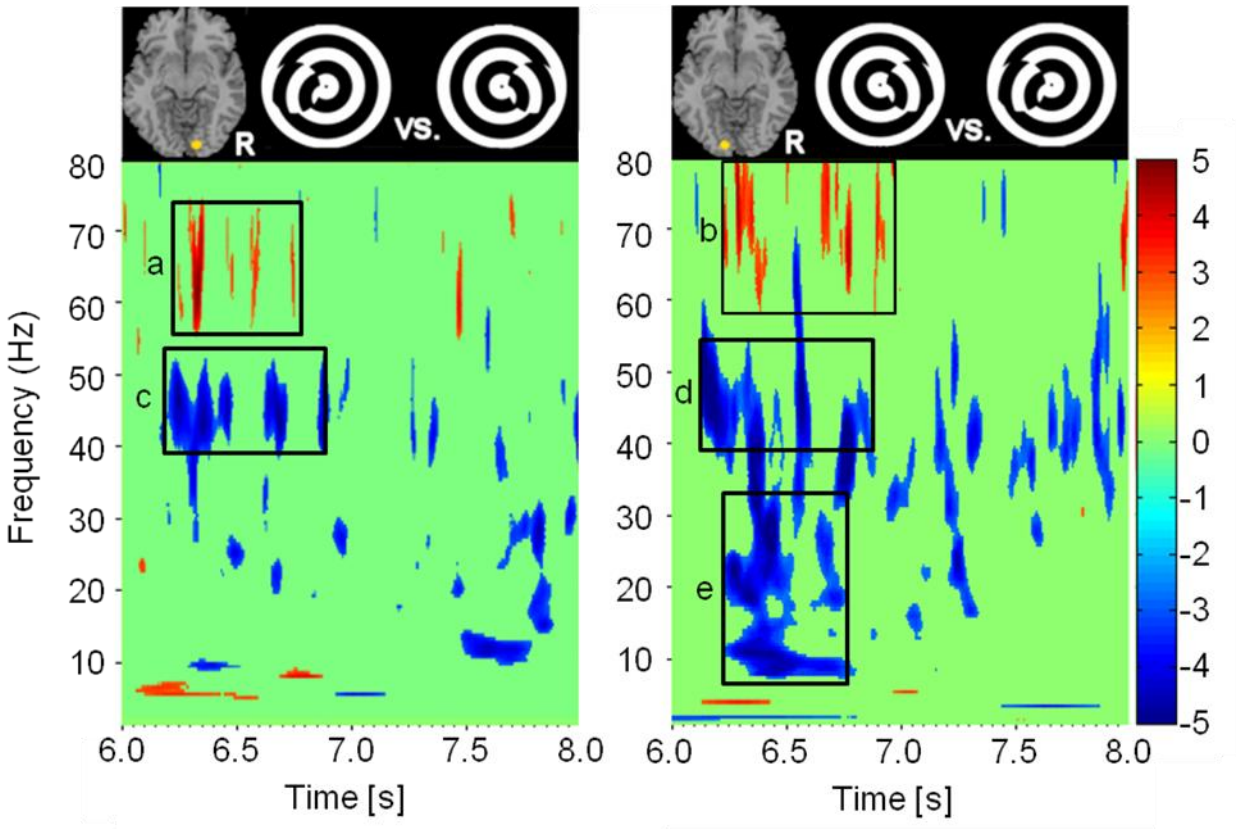
R
vs.
R
vs.
a
b
c
d
e
Frequency (Hz)
80
70
60
50
40
30
20
10
6.0
6.5
7.0
7.5
8.0
Time [s]
Time [s]
5
4
3
2
1
0
-1
-2
-3
-4
-5

Figure 4

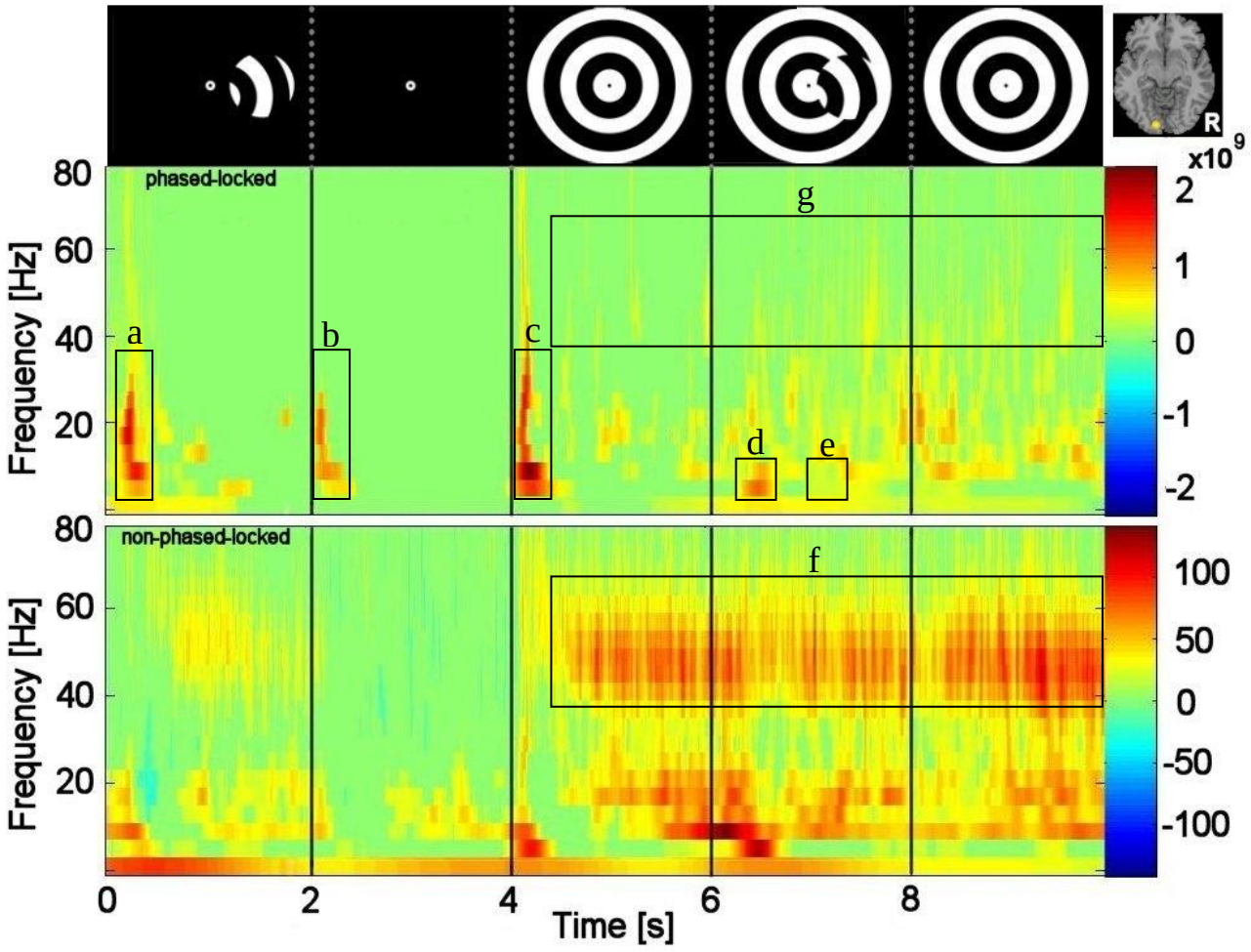
phased-locked
non-phased-locked
Frequency [Hz]
Time [s]
a
b
c
d
e
f
g
R
x10^9

Figure 5

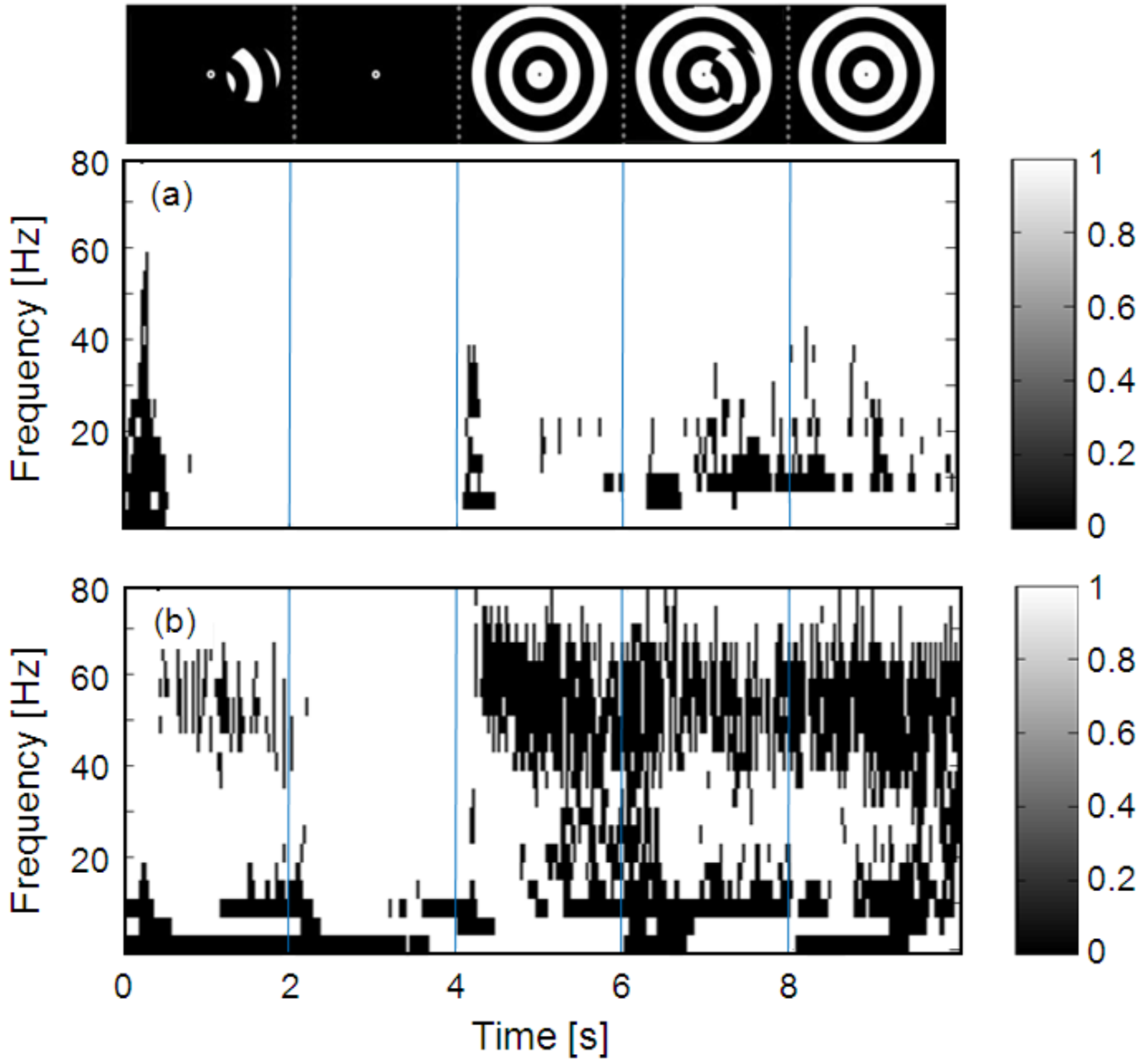
(a)
(b)
Frequency [Hz]
Frequency [Hz]
80
60
40
20
1
0.8
0.6
0.4
0.2
0
0
2
4
6
8
Time [s]

Figure 6